Grain boundary and triple junction enthalpies in nanocrystalline metals

A. Caro*
Centro Atómico Bariloche, 8400–Bariloche, Argentina

H. Van Swygenhoven†
Paul Scherrer Institute, 5232 Villigen, Switzerland

(Received 22 September 2000; published 27 February 2001)

We calculate the contribution to the total enthalpy of nanocrystalline computer-generated samples coming from grain boundaries, (GB's) and triple joints (TJ's). We show that the excess enthalpy per unit volume (excess enthalpy density) at the TJ is essentially the same as that found in the GB. This implies that TJ's and GB's are kinds of matter with equivalent departures from a perfect crystal structure, at least in the energetic aspect. By a proper account of the amount of GB's and TJ's, we show that the reported observations on decreasing GB energy with decreasing grain size in nanocrystallized amorphous Se [K. Lu and N. X. Sun, Philos. Mag Lett. **75**, 389 (1997)] and negative TJ line tension from computer simulation results [S. G. Srinivasan *et al.*, Acta Mater. **47**, 2821 (1999)] are consequences of neglecting the relation between the grain boundary width δ and the grain size d, which in the nanophase regime may be of the same order of magnitude.

DOI: 10.1103/PhysRevB.63.134101 PACS number(s): 81.07.−b, 61.72.Mm, 02.70.Ns, 68.35.Ct

The development of nanocrystalline (NC) materials opened the possibility to study structural and energetic properties of crystalline materials characterized by a large portion of interfaces. Knowledge on the nature of grain boundaries (GB's) in NC materials is essential to understand, develop, and eventually utilize this class of materials. Fundamental studies of GB properties were carried out on NC materials as well as on specially prepared polycrystals with chosen parameters. These studies, either experimental or computational, focused on several complementary aspects, like interface migration,[1] stress calculations,[2–4] anisotropic grain growth,[5] relaxation modes,[6] structure,[7,8] etc.

Experiments and computer simulations contribute to these issues together. In a recent paper[9] we showed that computer simulations of Cu and Ni NC samples indicate that GB structures are quite similar to those corresponding to coarser grains, supporting the interpretation of GB's in NC materials as similar to normal, micrometer-sized, polycrystals. These conclusions came from observation of the atomic arrangements at the interfaces.

Another way to look at the interfaces is by energetic considerations. When compared to their single-crystal counterpart, NC materials have an excess enthalpy per unit volume ΔH, defined as the difference between the enthalpy of the NC state minus the enthalpy of the perfect crystalline state at the same temperature and pressure. This difference is proportional to the energy stored in structural defects, like GB's, and triple joints (TJ's). Experimentally, this excess enthalpy can be measured as the heat released during grain growth, in a differential scanning calorimetric experiment (DSC); in computer experiments this quantity is of immediate access.

In this paper we report results on GB and TJ excess enthalpy on a set of NC samples that have already been used to study their elastic and mechanical properties.[9–11] We focus our attention on their dependence on average grain size, and compare our results with recent papers that claim a decrease in excess enthalpy as the grain size decreases,[12,13] or a negative TJ enthalpy.[14] The paper is organized as follows: first the model for defect counting is presented; second we fit it to our previous excess enthalpy results; then we reanalyze the results of Refs. 13 and 14 in terms of our model; and finally we present the conclusions.

I. MODEL

Although real as well as computer generated NC samples are formed by grains of arbitrary shape, to evaluate the amount of GB area and TJ length when the only macroscopic parameter is the average grain size, we must assume a particular shape and a size distribution. It is customary to take an average of the actual distribution of shapes and sizes that translates into a geometric factor representing the average surface-to-volume ratio. This factor alters the quantitative results of defect energies, but not their dependence on relevant variables like grain size. For simplicity, in our analysis of the computer-generated samples, instead of an average we shall assume two extreme geometries, namely, spherical (with minimum surface to volume ratio) and cubic (with large surface to volume ratio); the real case will very probably be in between these two cases. This simplification allows us to calculate the amount of defect surface or length with precision.

For simplicity, then, we consider a NC formed by perfectly equal cubes. The NC sample would then look like Fig. 1, with additional grains perpendicular to the plane of the figure. In the schematic figure, the grain size d is the sum of the size of the perfect crystal portion of the grain, $d-\delta$, plus the GB width δ. We assume (and justify below) that as d changes, δ remains constant.

The TJ is the intersection of three-grain boundaries. For this particular example of cubic grains, all intersections are four-junction line. Six-junction points may be identified in the intersection of six four-junction lines and so on: for each particular geometry considered, there are different types of intersections. In our analysis, we shall classify the defects in

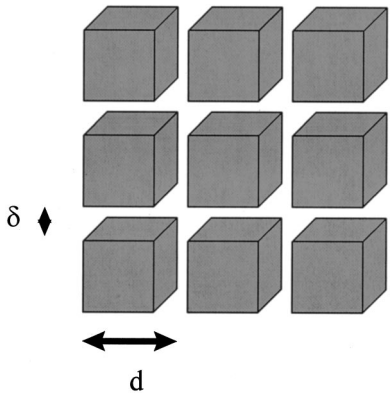

FIG. 1. Simplified representation of a nanophase material: cubic grains with linear dimension d and grain boundary width δ.

such a way that the volume associated with the six-junction points will be included in the four-junction lines, so they will not be considered as independent defects; moreover, we shall call them all TJ's. As a very important point in all that follows, note that there are several options to count the amount of defects: for the cubic shape example they can be GB's alone, GB's plus four-junction lines, and GB's plus four-junction lines plus six-junction lines. In Sec. III we shall consider GB's only, to compare with results in the literature. These options are not all equivalent: the results depend significantly on them as we show below.

With these definitions, the grain density n_g, that is, the number of grains per unit volume, is the reciprocal of the grain volume V_g. For a general shape, $V_g = g d^3$, with $g = 1$ for cubic shapes and $g = 0.52$ for spherical shapes. Then for cubes,

$$n_g = \frac{1}{V_g} = \frac{1}{d^3}. \tag{1}$$

The GB surface per unit volume S_{GB} is the surface of a grain S_g times the number of grains per unit volume n_g, times $\frac{1}{2}$ for double counting because each surface is shared by two grains. The surface of a grain is $g'(d-\delta)^2$, with $g' = 6$ for cubic and $g' = 3.14$ for spherical shapes; then

$$S_{\mathrm{GB}} = n_g S_g = \frac{6(d-\delta)^2}{2d^3}. \tag{2}$$

The TJ's length per unit volume (including eight-point junctions for our simplified geometry), l_{TJ}, is the product of the amount of TJ per grain, times the number of grains per unit volume. The first quantity is proportional to the linear dimensions of the grain, $g'' d$. In the case of cubic grains $g'' = 12$, and to avoid multiple counting (in cubic grains the TJ's are four-junction lines, shared by four nearest-neighbor grains), we add a factor $\frac{1}{4}$:

$$l_{\mathrm{TJ}} = n_g g'' d = \frac{12d}{4d^3} = \frac{3}{d^2}. \tag{3}$$

Note here that if we want to make the six-joint lines appear explicitly in the analysis as a separate term, $g'' d$ should be replaced by $g''(d-\delta)$ in the expression for l_{TJ}, and an additional expression for the amount of six-joint lines should be considered. With these definitions, the excess enthalpy per unit volume is

$$\Delta H = \gamma_{\mathrm{GB}} S_{\mathrm{GB}} + \gamma_{\mathrm{TJ}} l_{\mathrm{TJ}}, \tag{4}$$

where γ_{GB} and γ_{TJ} are the surface energy density of the GB and the length energy density of the TJ; replacing the surface and length densities by the expressions above,

$$\Delta H = \gamma_{\mathrm{GB}} 3 \frac{(d-\delta)^2}{d^3} + \gamma_{\mathrm{TJ}} \frac{3}{d^2}. \tag{5}$$

Neglecting terms in δ^2/d (because $\delta < d$), a plot of $\frac{1}{3} \Delta H d^2 \cong \gamma_{\mathrm{GB}} d + (\gamma_{\mathrm{TJ}} - 2\delta\gamma_{\mathrm{GB}})$ gives a straight line with slope γ_{GB}. To be able to determine the other two unknowns, γ_{TJ} and δ, and for reasons that will become clear later when inspecting the computer-generated samples, let us also assume that the states of matter in the GB and TJ are the same. These states may be characterized by an excess enthalpy per unit volume h. Then the enthalpy per unit surface of the GB is the enthalpy per unit volume of the defect matter, h, times the GB width δ. Similarly for the four-joint line, its enthalpy per unit length is $h\delta^2$; therefore $\gamma_{\mathrm{GB}} = h\delta$ and $\gamma_{\mathrm{TJ}} = h\delta^2$, and Eq. (5) now reads,

$$\begin{aligned} \Delta H &= h\delta \frac{3(d-\delta)^2}{d^3} + h\delta^2 \frac{3}{d^2} \\ &= \frac{3h\delta}{d}\left(1 - \frac{\delta}{d} - \frac{\delta^2}{d^2}\right) \\ &\cong \frac{3h\delta}{d^2}(d-\delta); \end{aligned} \tag{6}$$

here again we neglect terms higher than linear in δ/d. Now multiplying ΔH times d^2 we obtain a linear dependence on d with slope $3h\delta$ and intersection $-h\delta^2$ (note the negative sign). This allows us to determine both unknowns h and δ:

$$\Delta H d^2 = 3h\delta d - 3h\delta^2. \tag{7}$$

II. RESULTS

We apply Eq. (7) to our computer simulation results on Ni samples at different grain sizes, reported in Refs. 9–11. For details about the samples we refer the reader to Ref. 16, and only mention here that they do not have cubic grains but grains constructed from random locations and crystallographic orientations, according to the Voronoi construction (Wigner-Seitz cells). In Table I we give values of the excess enthalpy for the total sample of N_{at} atoms and average grain size d. The left ordinate axis of Fig. 2 shows $\Delta H d^2$ vs d, together with a linear fit [Eq. (7)] with: $3h\delta = 38.0(\pm 0.1)$ eV/nm^2 and $3h\delta^2 = 26.4(\pm 9)$ eV/nm. From these values, we determine $\delta = 0.7$ nm and $h = 18$ eV/nm^3 $= 0.21$ eV/at, $\gamma_{\mathrm{GB}} = h\delta = 12.6$ eV/nm$^2 = 2.0$ J/m^2, and $\gamma_{\mathrm{TJ}} = h\delta^2 = 8.8$ eV/nm $= 14.1 \times 10^{-10}$ J/m. The value of δ is compatible with the observed width of the GB determined in

TABLE I. Total excess enthalpy ΔH in samples with different grain sizes d. The number of atoms in the samples are also reported for normalization purposes.

ΔH (eV)	d (nm)	N_{at}
7 294	5.2	101 384
17 420	8.0	349 545
29 650	10.0	755 475
41 341	12.0	1 223 250

the simulations; and h is close to the latent heat of melting of this potential (0.18 eV/at), which is a measure of the energy necessary to lose the crystalline order.

The quality of the linear fit provides support to the defect accounting assumptions made, and unambiguously determines the GB energy. The assumption that the natures of the defect matter in the GB and TJ are similar gives us values for the TJ energy and the GB width, this last being compatible with the observations in the computer-generated samples, as shown below.

An additional test of these assumptions is the visual observation of the GB's and TJ's in the simulated samples. In previous publications,[9–11,15] we reported extensive studies on structural, elastic, and plastic properties of a series of nanophase samples representing Cu and Ni. Some of these samples were created starting from the same set of random grain location and crystallographic orientation, but with different grain sizes, in such a way that the same sets of boundaries appear in different samples, differing only in the length scale. In Figs. 3 and 4 we show partial views of two of these samples: three grains with the same orientation parameters in a 5.2-nm Ni sample and a 12-nm Ni sample. As becomes apparent, grains in both samples have equal shapes but different sizes.

As a way to visualize the perfect crystal component of the grain, we plot a closed surface containing in its interior all atoms with a fcc coordination up to fourth neighbors. In this and our previous work, we classify atoms according to their coordination; for a description of this analysis see Ref. 16. In

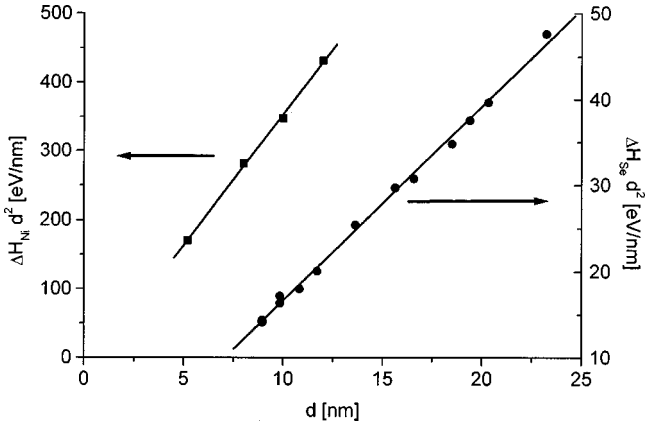

FIG. 2. The function ΔH times d^2 vs d. Left axis: our data for Ni from Ref. 15; right axis: Lu's data from Ref. 13. Linear fits according to Eq. (7).

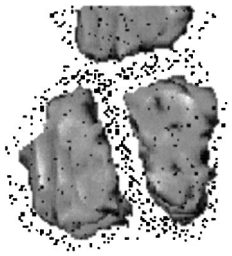

FIG. 3. Grain boundary and triple joint between three grains in a computer-generated 5.2-nm Ni NC sample. The surface of the grains has been taken as the frontier between perfect and nonperfect fcc-coordinated atoms. Small dots represent atoms with a potential energy greater than the perfect crystal value plus 1.5 times the latent heat of melting, as a way to visualize the excess energy stored in the defects.

the schematic representation of cubic grains shown in Fig. 1, and used in the calculations, this region has a characteristic linear dimension $d-\delta$. This is an arbitrary but sound definition of the frontier between a grain and a grain boundary, useful for visualization purposes. The perspective used in Figs. 3 and 4 clearly shows that the GB's are planar and constant in width, and that they intersect in a triple joint whose cross-section dimension is comparable to the GB width.

In addition to these surfaces, in Figs. 3 and 4 we also plot those atoms with an energy higher than 0.27 eV above the perfect crystal value. This value is 1.5 times the latent heat of melting, and is an arbitrary value that gives an adequate density of atoms in the figures to represent the distribution of excess enthalpy. It appears evident in Figs 3 and 4 that these atoms are evenly distributed in the GB and TJ volumes, with no distinction between a flat surface (what we associate to GB planes) and a dihedral vertex (that we associate with

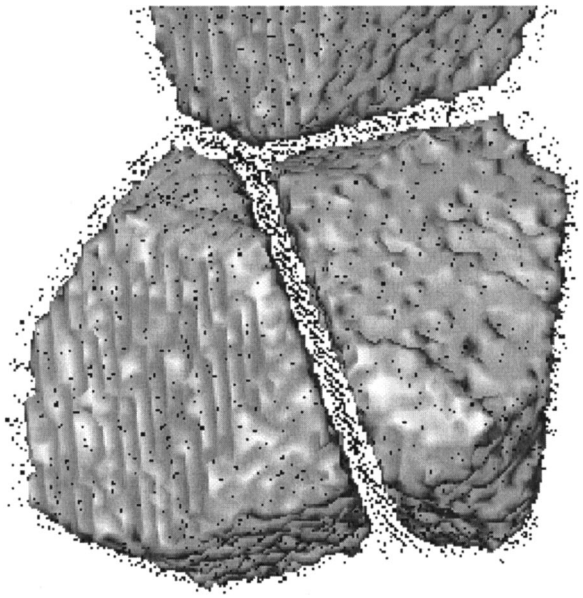

FIG. 4. Same as Fig. 3, this time for a computer-generated 12-nm Ni NC sample. The scale of this figure is the same as in Fig. 3

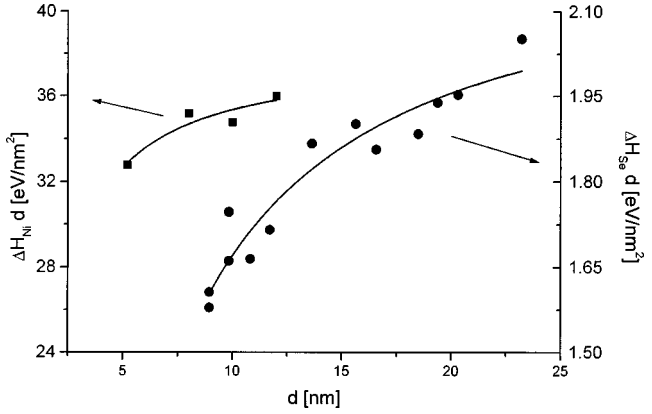

FIG. 5. Plot of ΔH times d vs d. Left axis: our data for Ni from Ref. 15; right axis: Lu's data from Ref. 13. Fits according to Eq. (8). This plot suggests a decrease in γ_{GB} as grain size d decreases.

TJ's). Also clear is the fact that for both grain sizes (12 and 5.2 nm), the width of the GB, that we call δ, and the density of energetic atoms, that is related to h in Eq. (6), are similar.

This average analysis suggests then that the nature of the GB in NC metals is quite independent of the grain size. However, it is only a small portion of the information that can be obtained from computer simulations. In fact, in a previous paper we presented an exhaustive analysis of particular GB's showing their structure and energetics depending on the missorientation parameters. In real experiments, however, it is this kind of average that is obtained from DSC measurements, while direct observation requires other, more sophisticated, techniques. These observations justify the assumptions made in Sec. I.

III. COMPARISON WITH OTHER WORKS IN THE LITERATURE

In a recent paper, Lu and Sun determined the excess enthalpy of NC selenium[13] obtained by recrystallization from the amorphous phase. Using the simple relation

$$\Delta H = \gamma_{GB} S_{GB}, \tag{8}$$

and $S_{GB}=3.34/d$, the authors determined γ_{GB} as $\gamma_{GB}=\Delta H/S_{GB}=\Delta H d/3.34$. If γ_{GB} is independent of d, a plot of ΔH times d versus d should give a constant horizontal line at $y=\gamma_{GB}$. Instead they obtained a line that has a negative curvature and a positive slope. They arrived at the conclusion that a significant decrease of the GB enthalpy as the grain size decreases indicates that the GB's nature depends on the grain size.

In view of the calculations presented in the preceding sections, we can interpret the conclusions of Lu and Sun as a consequence of a wrong account of GB area and energy balance in the NC phase. In fact the difference between Eqs. (5) and (8) is the origin of the dissimilar conclusion. Using our results from the simulations (Table I), and making a plot of ΔH times d versus d, we obtain the curve shown in the left ordinate axis in Fig. 5, which looks very similar to Lu and Sun's results, which are represented in the right ordinate axis. It appears evident that such a plot suggests a decrease in γ_{GB} as the grain size d decreases. However, the variable $\Delta H d$ should not be constant if we take Eq. (6) as the right expression for ΔH; for such a plot we instead obtain

$$\Delta H d = \frac{3h\delta}{d}(d-\delta) = 3h\delta\left(1-\frac{\delta}{d}\right), \tag{9}$$

which is a decreasing function of d. The lines in Fig. 5 are plots of Eq. (9) with δ and h for Ni, as determined previously, and for Se we obtain the same values as in the procedure indicated in the next paragraph.

For a proper determination of Se parameters, we represent Lu and Sun's data on the right ordinate axis in Fig. 2 in the spirit of Eq. (6), together with a fit to such Eq. (6). For these amorphous Se-annealed samples, we obtain that the GB width is 2.5 nm; and the GB energy is 0.4 J/m^2 assuming their geometric factor, and 0.36 J/m^2 assuming cubic grains. The GB width is significantly larger than in the metallic sample, but the difference may be due to the fact that Se samples are originally amorphous and grains grow by recrystallization. This procedure does not guarantee that the crystalline nucleus fills up all the volume. It is interesting to note that in the linear representation (Fig. 2) the data points show much less dispersion than in the nonlinear representation (Fig. 5). We believe that this provides support to the assumptions made in deriving Eq. (6); that is, the nature of the GB is independent of grain size. In summary, we conclude that the description given by Lu and Sun of the GB enthalpy does not correctly take into account the finite width of the GB, and therefore leads to an apparent decrease of the GB energy with decreasing grain size.

Another recent publication on computer simulations of TJ's, that also considers the grain boundary surface as proportional to d instead to $d-\delta$, is due to Srinivasan *et al.*[14] They concluded on a negative TJ enthalpy by the following enthalpy balance:

$$\Delta H = \gamma_{GB} S_{GB} + \gamma_{TJ} l_{TJ} = \frac{g'\gamma_{GB}}{d} + \frac{g''\gamma_{TJ}}{d^2}; \tag{10}$$

then

$$\Delta H d^2 = g'\gamma_{GB} d + g''\gamma_{TJ}. \tag{11}$$

In these expressions, g' and g'' are *positive* geometric constants. Equation (11) is used in Ref. 14 to calculate both γ's from the ΔH measured in simulations.

By comparing Eqs. (5)–(7) and (9) and (10), we know that multiplying ΔH times d^2 gives a straight line; this is what we already represented in Fig. 2. Interpreting the curves in Fig. 2 as a fit to Eq. (10), for Ni we obtain slope $g'\gamma_{GB}=38\,\mathrm{eV/nm^2}$ and a *negative* independent term $g''\gamma_{TJ}=-26.4\,\mathrm{eV/nm}$. Note that the negative sign in the independent term in Eq. (7) appears as a consequence of the $d-\delta$ variable used in the measure of surfaces. Instead, in Eq. (10) we obtain a negative value for a quantity that is assigned to the triple-line enthalpy. This led the authors of Ref. 14 to conclude that a negative line tension was obtained. In their discussion session, the authors of Ref. 14 clearly stated that a negative value is a consequence of the reference state con-

sidered, defined by the particular accounting method. We believe that our description of the defect length and area is clearer, as no negative energy densities appear.

IV. CONCLUSIONS

The computer simulations provide easy access to grain boundary enthalpies. The total excess enthalpy approach used here allows a direct comparison with experimental measurements on nanocrystalline samples. Our calculation suggests that since in the nanometer regime the GB width and grain size are of the same order of magnitude, a proper account of the amount of defects appearing in the enthalpy balance is essential to give a correct picture of the energetics involved. Moreover, our results show that the energy stored in the TJ's is the same kind of energy as stored in the GB's, and is related to the disorder that characterizes these regions; any other contribution, such as elastic deformation energy, gives values much lower than those associated to the disorder. This, in turn, allows us to reinterpret the experimental results of Lu and co-workers[11,12] and to provide numerical values for their NC Se GB surface enthalpy density and GB width. Additionally, we also reinterpret the results of Srinivasan *et al.*,[14] showing that concepts such as negative TJ enthalpy density are not necessary for the interpretation of their numerical simulations.

Computer simulations also provide more precise values of the GB excess enthalpy that do not require an assumption on the geometry of the grains. For each particular boundary we can define a region on a given GB plane, far from its boundaries, that is the portion of the GB that effectively divides two grains; that is, we can avoid contributions from triple or higher points. The energy of atoms in this fragment of the GB, together with those located in a volume inside both grains along the GB's normal direction, can be compared to the perfect crystal value to obtain the GB energy. In this way, we reported in Ref. 9 that a GB close to a low-energy twin has $\gamma_{GB}=1.1\,J/m^2$, while a highly disordered GB gives $\gamma_{GB}=1.6\,J/m^2$.

ACKNOWLEDGEMENTS

This research was supported by the Swiss National Science Fund, Grant No. 21-46832.96, and partially by CONICET Argentina PIP0664/98

*Electronic address: caro@cab.cnea.gov.ar
†Electronic address: helena.vs@psi.ch

[1] J. M. Huang and W. Yang, Modell. Simul. Mater. Sci. Eng. **7**, 87 (1999).
[2] S. X. Li, D. B. Ren, W. P. Jia, C. R. Chen, X. W. Li, and Z. G. Wang, Philos. Mag. A **80**, 1729 (2000).
[3] C. R. Chen, S. X. Li, J. L. Wen, and W. P. Jia, Mater. Sci. Eng. A **282**, 170 (2000).
[4] C. R. Chen and S. X. Li, Mater. Sci. Eng. A **257**, 312 (1998).
[5] N. M. Huang, J. Mater. Sci. **33**, 5625 (1998).
[6] K. L. Merkle, Microsc. Microanal. **3**, 339 (1997).
[7] O. A. Shenderova and D. W. Brenner, Phys. Rev. B **60**, 7053 (1999).
[8] X. Y. Qin, J. S. Zhu, L. D. Zhang, and X. Y. Zhou, J. Phys.: Condens. Matter **10**, 3075 (1998).
[9] H. Van Swygenhoven, D. Farkas, and A. Caro, Phys. Rev. B **62**, 831 (2000).
[10] H. Van Swygenhoven and A. Caro, Phys. Rev. B **58**, 11 246 (1998).
[11] H. Van Swygenhoven, M. Spaczer, A. Caro, and D. Farkas, Phys. Rev. B **60**, 22 (1999).
[12] K. Lu, R. Lück, and B. Predel, Scr. Metall. Mater. **28**, 1387 (1993).
[13] K. Lu and N. X. Sun, Philos. Mag. Lett. **75**, 389 (1997).
[14] S. G. Srinivasan, J. W. Cahn, H. Jónsson, and G. Kaloni, Acta Mater. **47**, 2821 (1999).
[15] H. Van Swygenhoven, M. Spaczer, and A. Caro, Acta Mater. **47**, 3117 (1999).
[16] J. D. Honeycutt and H. C. Andersen, J. Chem. Phys. **91**, 4950 (1987).